

Special relativity in a discrete quantum universe

Alessandro Bisio,^{*} Giacomo Mauro D'Ariano,[†] and Paolo Perinotti[‡]
Dipartimento di Fisica, Università di Pavia, via Bassi 6, 27100 Pavia, Italy
and Istituto Nazionale di Fisica Nucleare, Sezione di Pavia, Italy

(Received 10 June 2016; revised manuscript received 22 September 2016; published 20 October 2016)

The hypothesis of a discrete fabric of the universe, the “Planck scale,” is always on stage since it solves mathematical and conceptual problems in the infinitely small. However, it clashes with special relativity, which is designed for the continuum. Here, we show how the clash can be overcome within a discrete quantum theory where the evolution of fields is described by a quantum cellular automaton. The reconciliation is achieved by defining the change of observer as a change of representation of the dynamics, without any reference to space-time. We use the relativity principle, i.e., the invariance of dynamics under change of inertial observer, to identify a change of inertial frame with a symmetry of the dynamics. We consider the full group of such symmetries, and recover the usual Lorentz group in the relativistic regime of low energies, while at the Planck scale the covariance is nonlinearly distorted.

DOI: [10.1103/PhysRevA.94.042120](https://doi.org/10.1103/PhysRevA.94.042120)

I. INTRODUCTION

Is the world continuous or discrete? Feynman [1,2] motivated a discrete universe as the only way it can be simulated by its own constituents, which means by a quantum computer. Einstein himself considered a discrete space-time as a possibility, however, he complained about the lack of an appropriate mathematical framework [3]. Usually we dismiss discreteness on the basis of mathematical convenience of continuous theories. But, the continuum leads to still unsolved mathematical problems in the infinitely small, problems that do not arise in the discrete. The discrete, on the other hand, seems to raise an issue: the disagreement with Einstein’s special relativity.

The debate about the clash between a discrete space and Lorentz symmetry has been recently renewed because in some approaches to quantum gravity (such as Regge calculus [4], spin foam [5], causal sets [6]) the fundamental description of space-time is a discrete structure, to which the continuum is only an approximation. The scale of this discreteness is the Planck length, which is amazingly small: the Planck length compared to a meter is like the electron radius compared to the size of our galaxy.

Why would the Lorentz transformations not work with a discrete space-time? The objection is that a discrete space-time would not be invariant under the Lorentz group, even if we take it as discrete. Such a point, raised more than 60 years ago, was disproved for $d = 3$ space dimensions in Ref. [7]. However, it was shown that the minimum admissible boost would be huge: 0.866 times the speed of light! It seems therefore that there is no way for the reconciliation of Einstein’s special relativity with a discrete fabric of space-time. The issue is, however, a false problem, originating from the unnecessary requirement of enforcing a covariance designed for the continuum. The right point of view is to take the Lorentz covariance only as an approximate symmetry, and recovering it in the regime

where the discreteness looks continuous. This is similar to what happens for a crystalline medium, which looks isotropic at large scales, whereas instead it is highly anisotropic at microscopic scales. The smaller is the crystal structure, the more accurate is the continuum symmetry: think that the Planck length is 10^{-25} Å!

The right point of view is thus to consider the continuum as an approximation of the discrete when observed at very large scales. It is thus conceptually legitimate that the Lorentz transformations are actually distorted at the tiny Planck scale. An example of such a distorted Lorentz symmetry is that of *doubly special relativity* [8–10], where the distorted Lorentz transformations, in addition to the speed of light, preserve also an energy scale.

Here, we show that if we take only the very essence of the relativity principle, the invariance of the physical law under change of *inertial representation*, we get nonlinear Lorentz transformations, which happen to be of the same kind as those of doubly special relativity. In the continuum description, the reference frame is a Cartesian coordinate system, what is called “position representation” in quantum theory. Other representations of the dynamics are given in terms of constants of motion, such as the momentum or energy representations, and these provide a viable notion of inertial frame in a world made of countably many quantum systems.

II. QUANTUM WALK FROM PRINCIPLES

We take the pragmatic point of view that quantum theory is more efficient a description of our world than classical theory, pretty much like Kepler laws for the planet orbits are more efficient than Ptolemaic epicycles. We therefore consider the most general quantum discrete theory, which is a *quantum cellular automaton* [1,11,12]. This consists of infinitely many quantum systems (qubits, fermionic or bosonic fields), whose evolution occurs in discrete steps, and which interact *locally*, namely, every system interacts with a bounded number of other systems. A consequence of locality is that signals propagate at finite speed over the lattice of quantum systems. For our purposes, it is sufficient to consider a single particle, and technically this simplifies the automaton to be linear in the

^{*}alessandro.bisio@unipv.it

[†]dariano@unipv.it

[‡]paolo.perinotti@unipv.it

quantum field. Moreover, we require that the dynamics is reversible, hence, it is described by a unitary matrix: this is what is called *quantum walk* [13,14].

By denoting with G the set of the lattice's points we can conveniently introduce the Hilbert space $\ell^2(G)$ and the orthonormal basis $|\mathbf{x}\rangle$ which corresponds to the position of the particle. If we associate the Hilbert space \mathbb{C}^s to the internal degrees of freedom of the particle, the quantum walk (QW) is then a unitary operator on $\ell^2(G) \otimes \mathbb{C}^s$.

(a) *Locality*. The QW evolution is assumed to be *local*, i.e., information propagates through the lattice at a bounded speed. Given a lattice, let $N_{\mathbf{x}}$ be the set of nearest neighbors of the site \mathbf{x} . If the particle is localized at site \mathbf{x} , then, after one step of the QW, it must be localized within a finite set $N_{\mathbf{x}}$. Such a locality condition introduces a notion of causal cone in the lattice.

(b) *Homogeneity*. The evolution is assumed to be *homogeneous*, i.e., requirement that all the sites are equivalent. The QW evolution should not allow one to discriminate between two points \mathbf{x} and \mathbf{x}' . This requirement (see Ref. [15] for a full derivation) implies that the set of points G is a group and the lattice is a possible Cayley graph of this group.

(c) *Isotropy*. The assumption of *isotropy* translates the requirement that there is no privileged direction on the lattice. The mathematical translation of this requirement requires the existence of a group of permutations that act on the generators of the group G that can be faithfully represented on the internal degrees of freedom (see Ref. [15] for a full derivation).

(d) *Flat and curved space*. The above sketched framework encompasses a broad variety of dynamics. In particular, depending on the properties of the group G , we can have a quantum dynamics on a generally curved space. If we are interested to make contact with special relativity, it is natural to restrict the scenario to QWs corresponding to dynamics on the flat Minkowski space-time. This requirement corresponds to assume the existence of a quasi-isometry between the Cayley graph (with the word metric) of the group G and the Euclidean space \mathbb{R}^3 [16]. This assumption implies that the Abelian group \mathbb{Z}^3 must be a subgroup of G with finite order. We can further restrict ourselves to the case in which G coincides with \mathbb{Z}^3 itself. The price to pay for this restriction is to add additional internal degrees of freedom (see Ref. [17] for a more complete discussion).

(e) *Fourier analysis*. If the group G is Abelian, it is convenient to study the dynamics in the Fourier transform basis $|\mathbf{k}\rangle := (2\pi)^{\frac{3}{2}} \sum_{\mathbf{x}} e^{i\mathbf{k}\cdot\mathbf{x}} |\mathbf{x}\rangle$. Since homogeneity condition implies that the QW commutes with the translations on the lattice, in the Fourier basis the QW operator can be written as

$$A = \int_B d^3\mathbf{k} |\mathbf{k}\rangle \langle \mathbf{k}| \otimes A_{\mathbf{k}}, \quad (1)$$

where B denotes the first Brillouin zone of the underlying lattice. The unitary constraint implies that $A_{\mathbf{k}}$ is unitary for every $\mathbf{k} \in B$ and the locality assumption implies that $A_{\mathbf{k}}$ is a matrix polynomial in $e^{i\mathbf{h}\cdot\mathbf{k}}$. Notice that due to the discreteness of the lattice, the QW is band limited in \mathbf{k} . The spectrum $\{e^{i\omega_{\mathbf{k}}^{(i)}}\}$ of the operator $A_{\mathbf{k}}$, and especially its *dispersion relation* that is the expression of the phases $\omega_{\mathbf{k}}^{(i)}$ as functions of \mathbf{k} , plays a crucial role in the analysis of the QW dynamics.

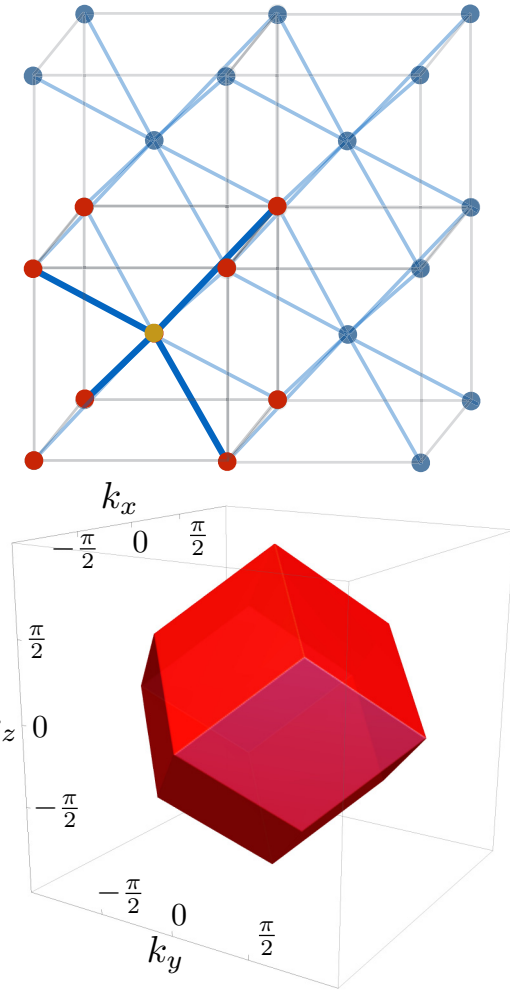


FIG. 1. Top: body-centered-cubic lattice. Each pair of nearest neighbor is connected by a blue link. Each point of the lattice has eight nearest neighbors, e.g., the red points are the nearest neighbors of the yellow one. Bottom: Brillouin zone B of the bcc lattice. The zone is a rhombic dodecahedron in which the opposite faces are identified.

(f) *Weyl quantum walk*. If the dimension of the Hilbert space of the internal degrees of freedom is $s = 2$ and the group G is \mathbb{Z}^3 , the requirements of *locality*, *homogeneity*, and *isotropy* then [15] the QWs can only be defined over the body-centered-cubic lattice and they are equivalent (up to a local change of basis) to the following two QWs:

$$\begin{aligned} A_{\mathbf{k}}^{\pm} &:= \lambda^{\pm}(\mathbf{k})I - i\mathbf{n}^{\pm}(\mathbf{k}) \cdot \boldsymbol{\sigma}^{\pm}, \quad (2) \\ \mathbf{n}^{\pm}(\mathbf{k}) &:= \begin{pmatrix} s_x c_y c_z \pm c_x s_y s_z \\ c_x s_y c_z \mp s_x c_y s_z \\ c_x c_y s_z \pm s_x s_y c_z \end{pmatrix}, \\ \lambda^{\pm}(\mathbf{k}) &:= (c_x c_y c_z \mp s_x s_y s_z), \quad (3) \\ c_{\alpha} &:= \cos(k_{\alpha}/\sqrt{3}), \quad s_{\alpha} := \sin(k_{\alpha}/\sqrt{3}), \quad \alpha = x, y, z. \end{aligned}$$

The Pauli matrices $\boldsymbol{\sigma}^{+} = \boldsymbol{\sigma}$ are the usual ones, while the $\boldsymbol{\sigma}^{-} = \boldsymbol{\sigma}^T$ are their transposed ones, and $\mathbf{k} \in B$ where B denotes the Brillouin zone of the bcc lattice (see Fig. 1).

III. CHANGE OF INERTIAL FRAME

Let us consider a quantum walk A as in Eq. (1) where the $A_{\mathbf{k}}$ are 2×2 matrices. The eigenvalues of A are obtained by solving the eigenvalue equation

$$A_{\mathbf{k}}\psi(\omega, \mathbf{k}) = e^{i\omega}\psi(\omega, \mathbf{k}) \quad (4)$$

which can be easily rewritten in relativistic notation as follows:

$$n_{\mu}(k)\sigma^{\mu}\psi(k) = 0, \quad (5)$$

where we introduced the four-vectors $k := (\omega, \mathbf{k})$, $n(k) := [\sin \omega, \mathbf{n}(\mathbf{k})]$, we defined $\sigma := (I, \sigma)$, and the vector $\mathbf{n}(\mathbf{k})$ is defined by

$$\mathbf{n}(\mathbf{k}) \cdot \sigma := \frac{i}{2}(A_{\mathbf{k}} - A_{\mathbf{k}}^{\dagger}). \quad (6)$$

The eigenvalues can be collected into two dispersion relations $\omega^{\pm}(\mathbf{k})$.

In this scenario, the constants of motions are \mathbf{k} and ω^{\pm} , hence, a change of representation corresponds to a map $k \mapsto k'(k)$. Then, the principle of relativity corresponds to the requirement that the eigenvalue equation (5) is preserved under a change of representation as follows:

$$n_{\mu}(k)\sigma^{\mu} = \tilde{\Gamma}_k^{-1} n_{\mu}(k')\sigma^{\mu} \Gamma_k, \quad (7)$$

where $\Gamma_k, \tilde{\Gamma}_k$ are invertible matrices. Equation (7) translates the relativity principle for the QW evolution: the dynamics is left invariant by a change of observer.

The simplest example of change of observer is the one given by the trivial relabeling $k' = k$ and by the matrices $\Gamma_k = \tilde{\Gamma}_k = e^{i\lambda(\mathbf{k})}$, where $\lambda(\mathbf{k})$ is an arbitrary real function of \mathbf{k} . When $\lambda(\mathbf{k})$ is a linear function, we recover the usual group of translations. The set of changes of representation $k \mapsto k'(k)$ for which Eq. (7) holds are a group, which is the largest group of symmetries of the dynamics.

IV. WEYL QUANTUM WALK AND SPECIAL RELATIVITY

Let us now apply this definition to the Weyl quantum walk of Eq. (2). The Weyl quantum walks have the remarkable feature that in the small wave-vector regime they recover, with the rescaling $\frac{\mathbf{k}}{\sqrt{3}} \rightarrow \mathbf{k}$, the two Weyl equations for the left- and right-handed massless fermions (hence their name). The dispersion relations of the two walks are given by

$$n_{\mu}^{\pm}(k)n^{\mu\pm}(k) = 0, \quad (8)$$

and are plotted in Fig. 2.

In the small wave-vector regime $\mathbf{k} \sim \mathbf{k}_0 = (0,0,0)$ one has $n(k) \sim k$, recovering the usual relativistic dispersion relation. The Weyl equations can be also recovered in the neighborhood of the wave vectors $\mathbf{k}_1 = \frac{\pi}{2}(1,1,1)$, $\mathbf{k}_2 = -\frac{\pi}{2}(1,1,1)$, $\mathbf{k}_3 = -\frac{\pi}{2}(1,0,0)$. The mapping between the vectors \mathbf{k}_i exchanges chirality of the particle and double the particles to four species in total. Therefore, we have four different particles (two left handed and two right handed), namely, the discreteness also doubles the particles, which is the well-known phenomenon of fermion doubling [18]. In the following, the term ‘‘small wave vector’’ will denote the neighborhoods of the vectors \mathbf{k}_i , $i = 0, \dots, 3$.

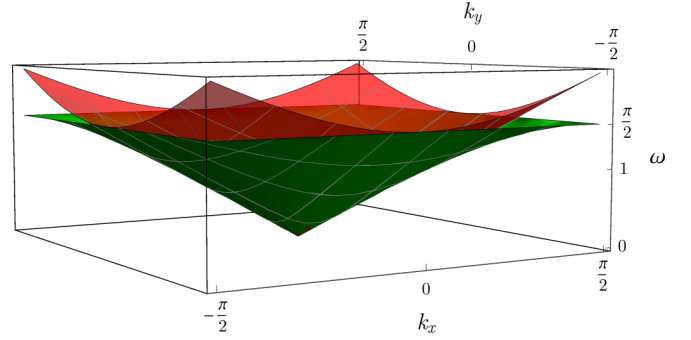


FIG. 2. The green surface represents the dispersion relation in Eq. (8) where we fixed $k_z = 0$ ($\omega_{\mathbf{k}} = \arccos \lambda^{\pm}(\mathbf{k})$ have the same plot). The red surface is the usual relativistic dispersion relation $\omega_{\mathbf{k}}^2 = k_x^2 + k_y^2$. Notice that the two surfaces get closer approaching the origin for $\mathbf{k} \rightarrow 0$.

We now show that the group of symmetries of the dynamics of the quantum walks in Eq. (2) contains a nonlinear representation of the Poincaré group, which exactly recovers the usual linear one in the small wave-vector regime.

For any arbitrary nonvanishing function $f(k)$ we can introduce the four-vector

$$p^{(f)} = \mathcal{D}^{(f)}(k) := f(k)n(k) \quad (9)$$

and rewrite the eigenvalue equation (5) as follows:

$$p_{\mu}^{(f)}\sigma^{\mu}\psi(k) = 0. \quad (10)$$

Let us now consider the following splitting of the Brillouin zone \mathbf{B} :

$$\begin{aligned} \mathbf{B}'_0 &:= \{\mathbf{k} \in \mathbf{B} | \lambda(\mathbf{k}) > 0, \cos(2k_y/\sqrt{3}) > 0\}, \\ \mathbf{B}'_1 &:= \{\mathbf{k} \in \mathbf{B} | \lambda(\mathbf{k}) < 0, \cos(2k_y/\sqrt{3}) > 0\}, \\ \mathbf{B}'_2 &:= \{\mathbf{k} \in \mathbf{B} | \lambda(\mathbf{k}) > 0, \cos(2k_y/\sqrt{3}) < 0\}, \\ \mathbf{B}'_3 &:= \{\mathbf{k} \in \mathbf{B} | \lambda(\mathbf{k}) < 0, \cos(2k_y/\sqrt{3}) < 0\}, \end{aligned} \quad (11)$$

with $\mathbf{B} = \cup_{i=0}^3 \mathbf{B}'_i$ up to a null-measure set, and let us denote with $\mathbf{n}^{(i)}(\mathbf{k})$ the restriction of $\mathbf{n}(\mathbf{k})$ to \mathbf{B}'_i . Notice that we dropped the label \pm denoting the two different Weyl walks since the results hold the same in the two cases. We now denote with \mathbf{U} the unit open ball in \mathbb{R}^3 ($\bar{\mathbf{U}}$ denotes its closure) and with \mathbf{H} the subset of \mathbf{U} defined as follows:

$$\mathbf{H} := \{\mathbf{m} \in \mathbf{U} \text{ such that } m_x = \pm m_z, 2m_x^2 + 2m_y^2 \geq 1\}. \quad (12)$$

We then consider the regions

$$\mathbf{B}_i := \mathbf{n}^{(i)-1}(\mathbf{U} \setminus \mathbf{H}) \quad (13)$$

and the function $f(\omega, \mathbf{k})$ defined as follows:

$$\begin{aligned} f(\omega, \mathbf{k}) &= g(\mathbf{n}(\mathbf{k})) \\ &= \tilde{g}(r, \theta, \phi) := 1 + r \int_0^r ds \left[\frac{1}{a(s)} + \frac{1}{b(s, \theta, \phi)} \right], \end{aligned} \quad (14)$$

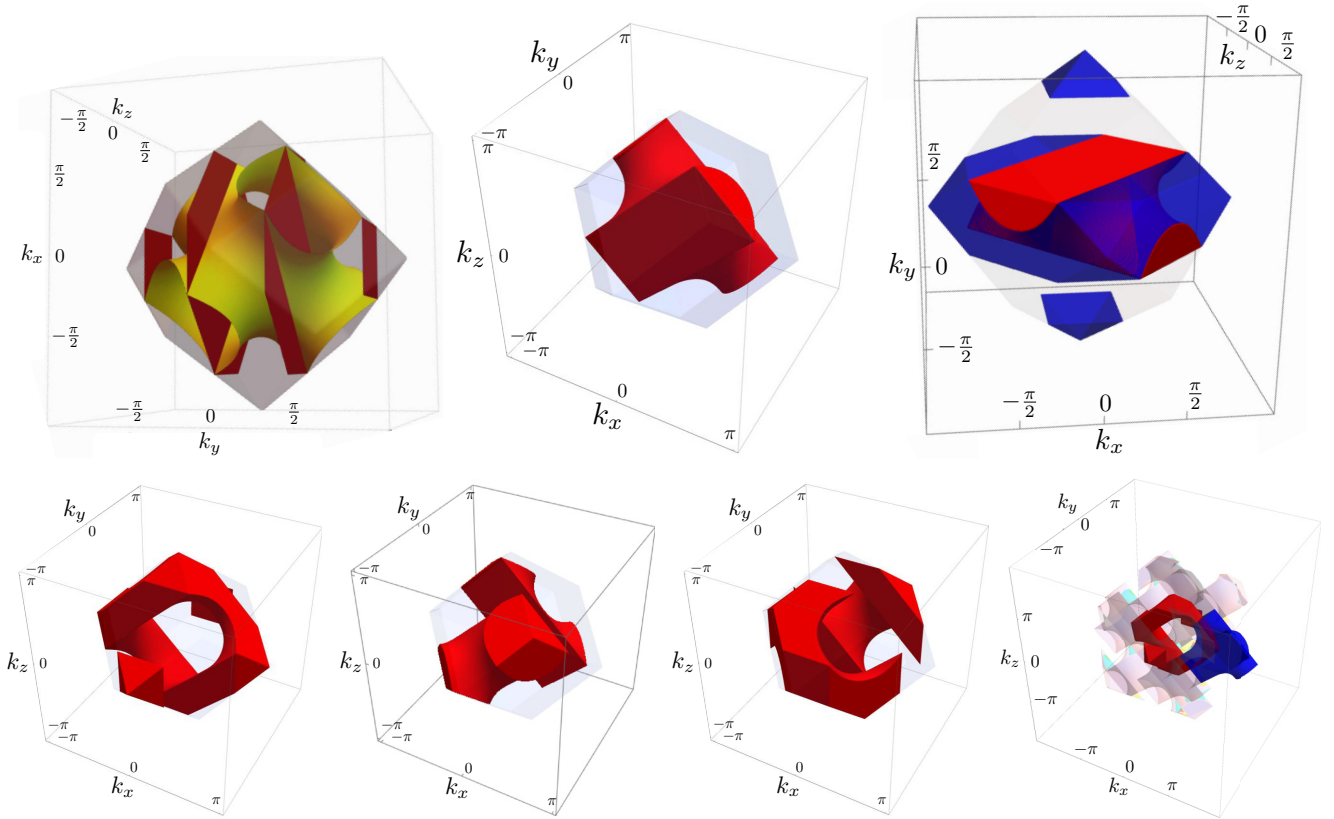


FIG. 3. Top left figure: surfaces $\lambda(\mathbf{k}) = 0$ in Eq. (3) (yellow) and $\cos(2k_y) = 0$ (red planes) inside the Brillouin zone (transparent). Top middle figure: \mathcal{B}_0 zone (red X shaped). Top right figure: \mathcal{B}_0 (red) and \mathcal{B}_1 (blue). Bottom left to right: $\mathcal{B}_1, \mathcal{B}_2, \mathcal{B}_3$. Bottom right: region \mathcal{B}_1 represented in a properly translated Brillouin zone. In this paper, the Lorentz transformations are those that leave the dispersion relations of the Weyl QW invariant, and act on the Weyl spinor independently of the wave vector. In such way they are nonlinear in (ω, \mathbf{k}) and linear over the Weyl spinor. Therefore, the Lorentz group acts as a group of diffeomorphisms over the Brillouin zone \mathcal{B} . The four domains $\mathcal{B}_i \subset \mathcal{B}$ are Lorentz invariant (up to a null-measure set, see Fig. 6 in the Appendix). More precisely, a point (ω, \mathbf{k}) with $\sin^2 \omega - |\mathbf{n}(\mathbf{k})|^2 = 0$ is mapped to a point (ω', \mathbf{k}') with $\sin^2 \omega' - |\mathbf{n}(\mathbf{k}')|^2 = 0$ and $\mathbf{k}' \in \mathcal{B}_i$. Moreover, the map \mathbf{n} maps each \mathcal{B}_i into the same set (up to null-measure set; see Fig. 6). Since the kinematics of a wave vector \mathbf{k} depends only on the vector $\mathbf{n}(\mathbf{k})$, we can conclude that the \mathcal{B}_i regions are kinematically equivalent and they can be interpreted as four different massless Weyl fermions. Because of the identification of the boundary points in the Brillouin zone, all the \mathcal{B}_i regions have the same X shape as \mathcal{B}_0 . This is evident in the bottom right figure, in which we see that the region \mathcal{B}_1 (in red), when represented in a properly translated Brillouin zone (in blue), has the same X shape as the region \mathcal{B}_0 . Considering the identification of the boundary points of the Brillouin zone in Fig. 1, one realizes that the opposite arms of the X are glued together, resulting in a solid double-torus (genus two). This result is rigorously proved in the Appendix where we show that the \mathcal{B}_i regions are diffeomorphic to a solid ball pierced by two arches of ellipses (Fig. 6 in the Appendix).

where

$$\begin{aligned} a(r) &:= 1 - r^2, \\ b(r, \theta, \phi) &:= [\cos^2(\phi) - \sin^2(\phi)]^2 \\ &\quad + \left\{ \frac{1}{2} - r^2 [1 - \cos^2(\theta) \sin^2(\phi)] \right\}^2, \end{aligned}$$

where we used the spherical coordinates $n_x(\mathbf{k}) = r \cos \theta \cos \phi$, $n_y(\mathbf{k}) = r \sin \theta$, $n_z(\mathbf{k}) = r \cos \theta \sin \phi$. Finally, we define the maps $\mathcal{D}^{(i)}$ as

$$\begin{aligned} \mathcal{D}^{(i)} : \Sigma_i &\rightarrow \Gamma_0, \quad \mathcal{D}^{(i)} : \begin{pmatrix} \omega \\ \mathbf{k} \end{pmatrix} \mapsto f(\omega, \mathbf{k}) \begin{pmatrix} \sin \omega \\ \mathbf{n}^{(i)}(\mathbf{k}) \end{pmatrix}, \\ \Sigma_i &:= \{(\omega, \mathbf{k}) \text{ such that } \mathbf{k} \in \mathcal{B}_i, \sin^2 \omega - |\mathbf{k}|^2 = 0\}, \\ \Gamma_0 &:= \{p \in \mathbb{R}^4 \text{ such that } p_\mu p^\mu = 0\}. \end{aligned} \quad (15)$$

One can prove (see Appendix A) that the maps $\mathcal{D}^{(i)}$ define an analytic diffeomorphism between Σ_i and Γ_0 . As a consequence, the composition

$$\mathcal{L}_\beta^{(i)} : \Sigma_i \rightarrow \Sigma_i, \quad \mathcal{L}_\beta^{(i)} := \mathcal{D}^{-1} \circ L_\beta \circ \mathcal{D} \quad (16)$$

is a well-defined nonlinear representation of the Lorentz group on the set Σ_i . Since the union of the \mathcal{B}_i sets coincides with the whole (up to a null-measure set) Brillouin zone (see Fig. 3), we have that the collection of the maps $\mathcal{L}_\beta^{(i)}$ provides a notion of Lorentz transformation for any (up to a null-measure set) solution of the Weyl QW dynamics.

The four invariant regions corresponding to the four different massless fermionic particles showing that the notion of “particle” as invariant of the Poincaré group survives in a discrete world, consistent with a physical interpretation of the fermion-doubled particles. For fixed function f the maps

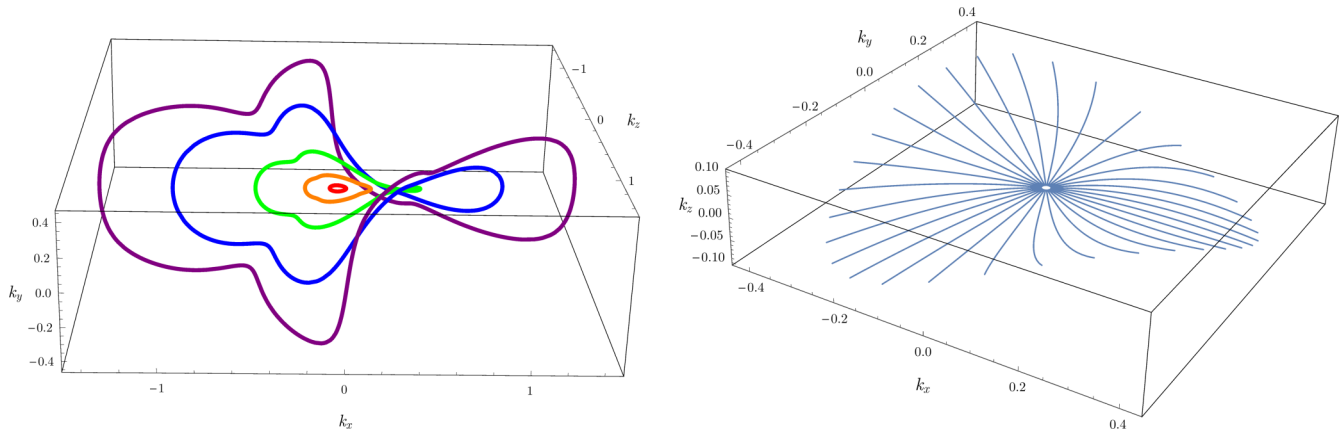


FIG. 4. The distortion effects of the Lorentz group for the discrete Planck-scale theory represented by the quantum walk in Eq. (2). Left figure: the orbit of the wave vectors $\mathbf{k} = (k_x, 0, 0)$, with $k_x \in \{0.05, 0.2, 0.5, 1, 1.7\}$ under the rotation around the z axis. Right figure: the orbit of wave vectors with $|\mathbf{k}| = 0.01$ for various directions in the (k_x, k_y) plane under the boosts with β parallel to \mathbf{k} and $|\beta| \in [0, \tanh 4]$.

$\mathcal{L}_\beta^{(f)}$ provide a nonlinear representation of the Lorentz group [9,10,19]. In Figs. 4 and 5, we show the numerical evaluation of some wave-vector orbits under subgroups of the nonlinear Lorentz. The distortion effects due to underlying discreteness are evident at large wave vectors and boosts. The relabeling $k \rightarrow k'(k) = \mathcal{L}_\beta^{(f)}(k)$ satisfies (7) with $\Gamma_k = \Lambda_\beta$ and $\tilde{\Gamma}_k = \tilde{\Lambda}_\beta$ for the right-handed particles, and $\Gamma_k = \tilde{\Lambda}_\beta$ and $\tilde{\Gamma}_k = \Lambda_\beta$ for the left-handed particles, with Λ_β and $\tilde{\Lambda}_\beta$ being the $(0, \frac{1}{2})$ and $(\frac{1}{2}, 0)$ representations of the Lorentz group, independently on k in each pertaining region.

For varying f , we obtain a much larger group, including infinitely many copies of the nonlinear Lorentz one. In the small wave-vector regime, the whole group collapses to the usual linear Lorentz group for each particle.

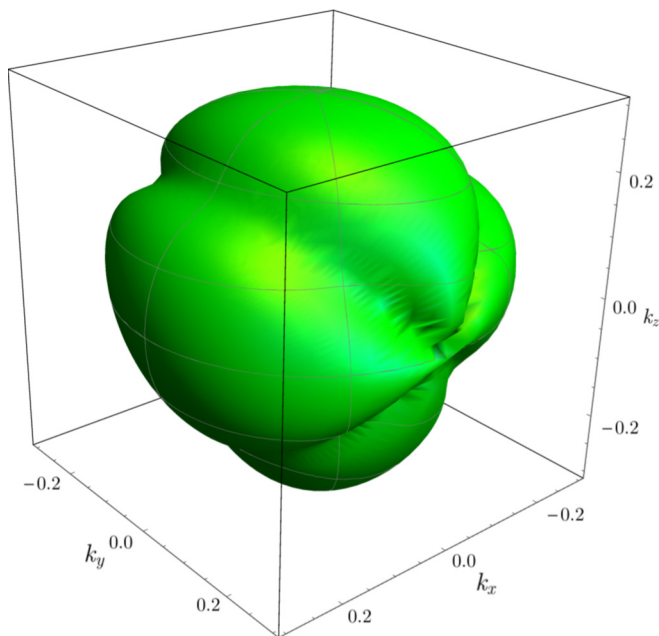


FIG. 5. The green surface represents the orbit of the wave vector $\mathbf{k} = (0.3, 0, 0)$ under the full rotation group $SO(3)$.

V. SPECIAL RELATIVITY AND THE DIRAC QUANTUM WALK

Up to now we have analyzed what happens with massless particles. A simple way to obtain the Dirac equation is to pair an automaton in Eq. (2) with its adjoint into a direct sum. As proved in Ref. [15], there are only two admissible quantum walks

$$D^\pm = \begin{pmatrix} nA^\pm & imI \\ imI & nA^\pm \end{pmatrix}, \quad (17)$$

$$0 \leq n, m \leq 1, \quad n^2 + m^2 = 1$$

giving the Dirac equation in the small wave-vector regime. A relevant feature of the discreteness is that because of unitarity the mass parameter is upper bounded [20].

The eigenvalue equation of the Dirac QW can be written as

$$[p_\mu^{(f)}(\omega, \mathbf{k}, m)\gamma^\mu - mI]\psi(\omega, \mathbf{k}, m) = 0, \quad (18)$$

where γ^μ are the Dirac γ matrices in the Weyl representation, and m is then interpreted as the particle mass. Due to the explicit dependence of $p_\mu^{(f)}$ from m the covariance under change of reference cannot leave the value of m invariant. In such case the dispersion relation resorts to the conservation of the de Sitter norm

$$\sin^2 \omega - (1 - m^2)|\mathbf{n}(\mathbf{k})|^2 - m^2 = 0. \quad (19)$$

The group leaving Eq. (19) invariant is the de Sitter group $SO(1,4)$. In the limit of $m \ll 1$, the usual Lorentz symmetry is recovered. The analysis of de Sitter covariance of Eq. (18) will be given in a forthcoming publication.

VI. CONCLUSION

We have seen what happens of the Lorentz group in a quantum world that is discrete. The main point is to abandon the idea of enforcing the exact Lorentz symmetry on the discrete, but instead to consider the symmetry as an approximate one that holds only in the small wave-vector and small mass regime. Within the framework of quantum cellular automata (QCA), the paradigmatic example of quantum dynamics on

a discrete set of systems, reasonable assumptions of algorithmic simplicity single out a QCA dynamics that recovers a Lorentz-invariant dynamics in a small wave-vector regime. The relativity principle is then stated as the invariance of the physical law under change of inertial representation and leads to nonlinear Lorentz transformations, as the ones considered in the doubly special relativity literature. This perspective is the reverse of the usual one, where the preexisting notions of space-time and of inertial frame of reference constrain the admissible dynamical laws to be covariant under the Poincaré group. In our approach, the dynamics, which derives from principles of computational nature, constrains the symmetries of the emerging space-time.

A reverse approach to the one presented in this paper, i.e., from classical to quantum, has been recently presented in Ref. [21]. There, the authors show that a fundamental length scale and a discrete background lattice can emerge as a consequence of the quantization of a classical phase space, through a generalization of the canonical approach of geometric quantization. They show that a choice of quantum polarization (a choice of a maximally commutative $*$ subalgebra) for the Heisenberg algebra which respects its linear structure, corresponds to a lattice on the phase space and to an irreducible representation of the Heisenberg group on square-integrable quasiperiodic functions on a cell in phase space. Within this discrete framework, the action of continuous translation and continuous rotations induces a change in the choice of quantum polarization (which is considered observer dependent), thus reconciling the discrete lattice structure with the continuous symmetry. In this picture, the starting point is a notion of a classical phase space endowed with classical symmetries whose action on the quantum operators can be defined through the Weyl map. The emergence of a minimal length and an observer-dependent notion of space-time are both consequences of the quantization and the choice of the quantum polarization.

One could now wonder how small is such an intrinsic discreteness scale. According to common opinion, the scale of discreteness a is identified with the Planck scale. In terms of the maximum wave vector k_M in the Brillouin zone, one has $k_M = \frac{\sqrt{3}\pi}{a}$. In the small wave-vector regime, we recover the simple relations [20] $c = \frac{a}{\sqrt{3}\tau}$ and $\hbar = \mu a c$, with c , \hbar , and τ denoting the speed of light, the Planck constant, and the time step, respectively. Then, the maximum mass μ of the quantum walk is the Planck mass.

The crucial question is now what can be actually seen experimentally. Recently, experimental tests of Planck-scale phenomenology have been proposed [22–24]. In particular, the modification to the usual dispersion relations can in principle be detected in observation of gamma-ray bursts from deep-space events, where billions of light years of distance can sufficiently amplify the weak vacuum dispersive behavior due to discreteness [25]. In our context, this can be proved with the free electromagnetic field derived as the two-particle sector of the quantum walk in Eq. (2) [26]. This possibility reconnects with the recent analysis of data [27] from Fermi-LAT concluding that the observations set an upper bound to the scale of discreteness which is smaller than the Planck scale a by a factor 2.8. The analysis of Ref. [27]

can be refined with a complete theoretical derivation based on Ref. [26] and on the results presented in this paper. This would also take into account the possibility of a compensating effect due to the phenomenon of relative locality [28]. In short, relative locality is the phenomenon due to the nonlinearity of the Lorentz transformations, which generalizes the relativity of simultaneity to relativity of the full space-time coincidence of events. The separation of events under boost is amplified by the difference of their frequency domain. Indeed, the Fermi-LAT observation is based on a predicted time delay between two events with a huge difference in frequency, which could then be compensated by the relative-locality effect. The fully fledged discrete theory given here, derived from very general principles, allows for a thorough quantitative evaluation that takes into account both the dispersive vacuum and nonlinear Lorentz transformations.

ACKNOWLEDGMENT

This work has been supported by the Templeton Foundation under the Project No. 43796, *A Quantum-Digital Universe*.

APPENDIX A: DEFORMED RELATIVITY FOR THE WEYL QUANTUM WALK

In this appendix, we prove that the construction in Eq. (A13) is a well-defined deformed Lorentz symmetry for each set Σ_i . In the following, we will adopt the convention $\frac{\mathbf{k}}{\sqrt{3}} \rightarrow \mathbf{k}$, in order to lighten the notation by getting rid of the $\frac{1}{\sqrt{3}}$ factors.

Let us define

$$\begin{aligned} \mathcal{D} &= \mathcal{N} \circ \mathcal{P}, & \mathcal{P} &: (\omega, \mathbf{k}) \mapsto (\omega, \mathbf{n}(\mathbf{k})), \\ \mathcal{N} &: \begin{pmatrix} \omega \\ \mathbf{m} \end{pmatrix} \mapsto g(\omega, \mathbf{m}) \begin{pmatrix} \sin \omega \\ \mathbf{m} \end{pmatrix}, \end{aligned} \quad (\text{A1})$$

where we also assumed $f(\omega, \mathbf{k}) = g(\omega, \mathbf{n}(\mathbf{k}))$.

We now need to study separately the properties of the two maps \mathcal{P} and \mathcal{N} .

1. Study of the map $\mathbf{n}(\mathbf{k})$

In this section, we study the analytical properties of the map \mathcal{P} , which, according to Eq. (A1) resort to the map \mathbf{n} . The analysis will proceed through the determination of the largest subdomains $\{\mathcal{B}'_i\}$ of invertibility of the map \mathbf{n} . We first prove that on the closure $\bar{\mathcal{B}}_i$ of each domain the map is surjective on the closed unit sphere $\bar{\mathcal{U}}$. Then, we determine the geometry of the ranges $\mathbf{n}(\mathcal{B}'_i)$, showing that they are homotopic to a solid genus two-torus.

Let us denote by \mathcal{B} the Brillouin zone of the center cubic lattice. \mathcal{B} , upon a proper identification of its boundary points (see Fig. 1), is a compact three-dimensional manifold. The Jacobian $J_{\mathbf{n}}(\mathbf{k})$ of the map $\mathbf{n}(\mathbf{k})$ is given by

$$J_{\mathbf{n}}(\mathbf{k}) := \det[\partial_i n_j(\mathbf{k})] = \cos(2k_y)\lambda(\mathbf{k}), \quad (\text{A2})$$

and it vanishes on the set

$$\begin{aligned} \mathcal{F} &= \mathcal{G} \cup \mathcal{X}, \\ \mathcal{X} &:= \{\mathbf{k} \in \mathcal{B} \mid \cos(2k_y) = 0\}, \\ \mathcal{G} &:= \{\mathbf{k} \in \mathcal{B} \mid \lambda(\mathbf{k}) = 0\}. \end{aligned} \quad (\text{A3})$$

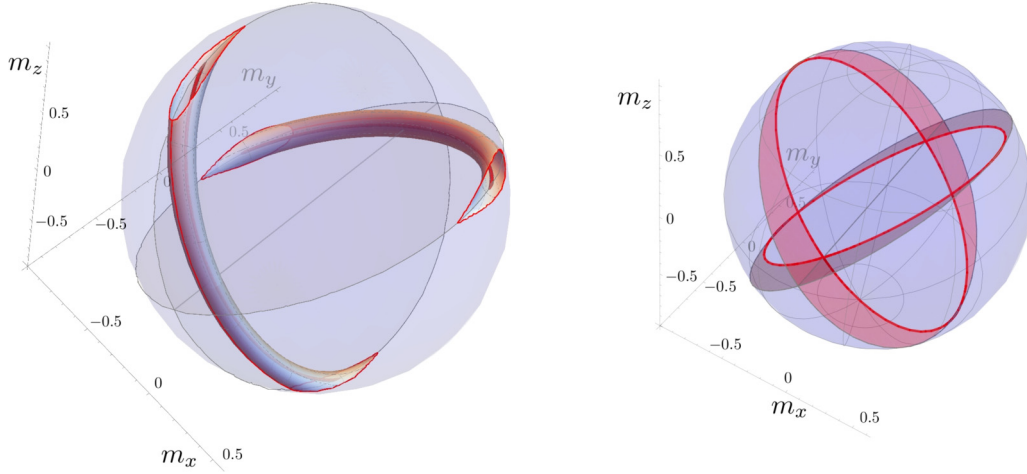


FIG. 6. Left figure: region Q_a . Right figure: H zone in red inside the unit ball. In the left figure, the tubes around the arches $\mathbf{e}_+(\mathcal{T}_1)$ and $\mathbf{e}_-(\mathcal{T}_2)$ emphasize the piercing of the ball by the one-dimensional holes along the elliptic arches $\mathbf{e}_+(\mathcal{T}_1)$ and $\mathbf{e}_-(\mathcal{T}_2)$. The region Q_a is clearly homeomorphic to a solid torus of genus two. Because of this nontrivial topological feature, the set $\{(\omega, \mathbf{m}) \text{ such that } |\omega| \leq \frac{\pi}{2}, \mathbf{m} \in \mathbf{n}(\mathcal{B}_i), \sin^2 \omega - |\mathbf{m}|^2 = 0\}$ cannot be diffeomorphic to any Lorentz-invariant region of \mathbb{M}^4 . However, it is possible to remove from the region Q_a a null-measure set such that the resulting topology is trivial. This can be done by removing the set H (red zones in the right figure), resulting in a star-shaped open set in \mathbb{R}^3 .

Since $\nabla \lambda(\mathbf{k}) \neq 0$ for all \mathbf{k} such that $\lambda(\mathbf{k}) = 0$, the implicit function theorem guarantees that \mathbf{G} is a well-defined two-dimensional surface. In the following, we will denote by $\{\mathcal{B}'_i\}$ (i ranging in some set) the disjoint connected subsets of $\mathcal{B} \setminus F$, thus,

$$\mathcal{B} \setminus F = \bigcup_i \mathcal{B}'_i, \quad \mathcal{B}'_i \cap \mathcal{B}'_j = \emptyset \text{ for } i \neq j. \quad (\text{A4})$$

For each i the set \mathcal{B}'_i is open and we denote as $\overline{\mathcal{B}'_i}$ its closure and as $\partial \mathcal{B}'_i$ its boundary.

Now, let us denote with $\overline{\mathcal{U}} \subset \mathbb{R}^3$ the closed unit-radius ball, and with \mathcal{S}^2 the sphere of radius 1 in \mathbb{R}^3 . Moreover, let us define the parametric curves

$$\mathbf{e}_\pm(t) := \frac{1}{\sqrt{2}}[\sin(t), \cos(t), \pm \sin(t)]^T \quad (\text{A5})$$

and the sets

$$\begin{aligned} Q_a &:= \mathcal{U} \setminus (\mathbf{e}_+(\mathcal{T}_1) \cup \mathbf{e}_-(\mathcal{T}_2)), \\ Q_b &:= \mathcal{U} \setminus (\mathbf{e}_+(\mathcal{T}_2) \cup \mathbf{e}_-(\mathcal{T}_1)), \\ \mathcal{T}_1 &:= \left(-\frac{\pi}{2}, \frac{\pi}{2}\right), \\ \mathcal{T}_2 &:= \left(-\pi, -\frac{\pi}{2}\right) \cup \left(\frac{\pi}{2}, \pi\right]. \end{aligned} \quad (\text{A6})$$

Given all the definitions introduced in this section, we have then the following result:

Lemma 1. Equation (A4) defines four regions \mathcal{B}'_i which are determined by the following conditions

$$\begin{aligned} \mathcal{B}'_0 &:= \{\mathbf{k} \in \mathcal{B} | \lambda(\mathbf{k}) > 0, \cos(2k_y) > 0\}, \\ \mathcal{B}'_1 &:= \{\mathbf{k} \in \mathcal{B} | \lambda(\mathbf{k}) < 0, \cos(2k_y) > 0\}, \\ \mathcal{B}'_2 &:= \{\mathbf{k} \in \mathcal{B} | \lambda(\mathbf{k}) > 0, \cos(2k_y) < 0\}, \\ \mathcal{B}'_3 &:= \{\mathbf{k} \in \mathcal{B} | \lambda(\mathbf{k}) < 0, \cos(2k_y) < 0\}. \end{aligned}$$

For each i , let $\mathbf{n}^{(i)}(\mathbf{k})$ denote the restriction of the map $\mathbf{n}(\mathbf{k})$ to the set \mathcal{B}'_i . Then, $\mathbf{n}^{(i)}(\mathbf{k})$ defines a diffeomorphism between \mathcal{B}'_i

and its image $\mathbf{n}^{(i)}(\mathcal{B}'_i)$ and we have

$$\begin{aligned} \mathbf{n}^{(0)}(\mathcal{B}'_0) &= \mathbf{n}^{(2)}(\mathcal{B}'_2) = Q_a, \\ \mathbf{n}^{(1)}(\mathcal{B}'_1) &= \mathbf{n}^{(3)}(\mathcal{B}'_3) = Q_b. \end{aligned} \quad (\text{A7})$$

The proof of this result is rather involved and can be found in Appendix B. The \mathcal{B}'_i regions are plotted in Fig. 3. The most important consequence of this result is that, for each i , the set $\mathbf{n}(\mathcal{B}'_i)$ (see Fig. 6) (i) coincides with \mathcal{U} except a null-measure set and (ii) it is homeomorphic to a genus two-torus.

2. Study of the map \mathcal{N}

Since for all i the region $\mathbf{n}(\mathcal{B}'_i)$ has a nontrivial topology, the set $\{(\omega, \mathbf{m}) \text{ such that } |\omega| \leq \frac{\pi}{2}, \mathbf{m} \in \mathbf{n}(\mathcal{B}'_i), \sin^2 \omega - |\mathbf{m}|^2 = 0\}$ cannot be diffeomorphic to any Lorentz-invariant region of \mathbb{M}^4 . A possible way to change the topology of $\mathbf{n}(\mathcal{B}'_i)$ is to exclude the set $H \subseteq \overline{\mathcal{U}}$ (as it is shown in Fig. 6) of vectors \mathbf{m} satisfying the following inequalities:

$$\begin{aligned} m_x &= \pm m_z, \\ 2m_x^2 + m_y^2 &\leq 1, \\ 2m_x^2 + 2m_y^2 &\geq 1. \end{aligned} \quad (\text{A8})$$

Then, the set $\mathcal{U} \setminus H$ is topologically trivial and we have $\mathcal{U} \setminus H \subset \mathbf{n}(\mathcal{B}'_i)$ for all i . Let us now consider the function $\mathcal{N} : (\omega, \mathbf{m}) \mapsto (p_0, \mathbf{p}) = g(\omega, \mathbf{m})(\sin \omega, \mathbf{m})$ restricted to the set

$$\begin{aligned} \mathcal{N} &:= \{(\omega, \mathbf{m}) \text{ such that } \mathbf{m} \in \mathcal{U} \setminus H, \\ &|\omega| \leq \frac{\pi}{2}, \sin^2 \omega - |\mathbf{m}|^2 = 0\}. \end{aligned} \quad (\text{A9})$$

As shown in Appendix C, it is possible to define the function $g(\omega, \mathbf{m})$ is such that \mathcal{N} defines a diffeomorphism between \mathcal{N} and the null mass shell

$$\Gamma_0 := \{p \in \mathbb{M}^4, \text{ such that } p^\mu p_\mu = 0\} \quad (\text{A10})$$

and that its Jacobian matrix at the origin is 0, i.e.,

$$J_{\mathcal{N}}(\mathbf{0}) = I. \quad (\text{A11})$$

Finally, for each i we denote by \mathbf{B}_i the counterimage of the set $\mathbf{U} \setminus \mathbf{H}$ under the map $\mathbf{n}^{(i)}$ and by $\mathcal{D}^{(i)}$ the composition

$$\mathcal{D}^{(i)} : \Sigma_i \rightarrow \Gamma_0, \quad \mathcal{D}^{(i)} := \mathcal{N} \circ \mathcal{P}^{(i)}, \quad (\text{A12})$$

$$\mathcal{P}^{(i)} : \Sigma_i \rightarrow \mathbf{N}, \quad \mathcal{P}^{(i)} : \begin{pmatrix} \omega \\ \mathbf{k} \end{pmatrix} \mapsto \begin{pmatrix} \omega \\ \mathbf{n}^{(i)}(\mathbf{k}) \end{pmatrix},$$

$$\mathcal{N} : \mathbf{N} \rightarrow \Gamma_0, \quad \mathcal{N} : \begin{pmatrix} \omega \\ \mathbf{m} \end{pmatrix} \mapsto g(\omega, \mathbf{m}) \begin{pmatrix} \sin \omega \\ \mathbf{m} \end{pmatrix},$$

$$\Sigma_i := \{(\omega, \mathbf{k}) \text{ such that } \mathbf{k} \in \mathbf{B}_i, \sin^2 \omega - |\mathbf{k}|^2 = 0\}.$$

For each i , the map $\mathcal{D}^{(i)}$ is an analytic diffeomorphism between the region Σ_i and the Lorentz-invariant set Γ_0 which satisfies the condition $J_{\mathcal{D}^{(i)}}(\mathbf{0}) = I$. Then, the composition

$$\mathcal{L}_\beta^{(i)} : \Sigma_i \rightarrow \Sigma_i, \quad \mathcal{L}_\beta^{(i)} := \mathcal{D}^{-1} \circ L_\beta \circ \mathcal{D} \quad (\text{A13})$$

is a well-defined nonlinear representation of the Lorentz group on the set Σ_i . Since the union of the \mathbf{B}_i sets coincides with the whole (up to a null-measure set) Brillouin zone, we have that the collection of the maps $\mathcal{L}_\beta^{(i)}$ provides a notion of Lorentz transformation for any (up to a null-measure set) solution of the Weyl QW dynamics.

APPENDIX B: PROOF OF LEMMA 1

In this appendix, we will give the proofs of the results contained in Lemma 1. Since the proof is quite involved, we split it into several pieces. Let us begin by defining the sets

$$\mathbf{Q}' := \bar{\mathbf{U}} \setminus \mathbf{R}, \quad \mathbf{R} := \mathbf{S}^2 \cup \mathbf{E}_+ \cup \mathbf{E}_-. \quad (\text{B1})$$

Obviously, \mathbf{Q}' is open and connected, with $\bar{\mathbf{Q}}' = \bar{\mathbf{U}}$ and $\partial \mathbf{Q}' = \mathbf{R}$. We now prove some useful properties of the map \mathbf{n} .

Sublemma 1. Let \mathbf{n}_i denote the restriction of the map \mathbf{n} to \mathbf{B}'_i . Then, for each i we have that \mathbf{n}_i is a diffeomorphism between \mathbf{B}'_i and $\mathbf{n}(\mathbf{B}'_i)$.

Proof. Since by definition $\mathbf{k} \in \mathbf{B}'_i \Rightarrow \mathbf{k} \notin \mathbf{F}$ we have $J_{\mathbf{n}}(\mathbf{k}) \neq 0$ for all $\mathbf{k} \in \mathbf{B}'_i$. Since \mathbf{B}'_i is connected and \mathbf{n} is analytical, we have the thesis. ■

Sublemma 2. We have the following inclusions:

- (1) $\mathbf{n}(\bar{\mathbf{B}}'_i) \subseteq \bar{\mathbf{U}}$,
- (2) $\partial \mathbf{n}(\mathbf{B}'_i) \subseteq \mathbf{R}$.

Proof. Let us start with the proof of item 1. By explicit computation, we have $|\mathbf{n}(\mathbf{k})|^2 = 1 - \lambda^2(\mathbf{k}) \leq 1$ which implies that the image of \mathbf{n} is contained in $\bar{\mathbf{U}}$.

We now prove item 2. Thanks to Lemma 1 we have that $\mathbf{n}(\mathbf{B}'_i)$ is open. On the other hand, since \mathbf{n} is continuous and $\bar{\mathbf{B}}'_i$ is compact, we have that $\mathbf{n}(\bar{\mathbf{B}}'_i)$ is compact and then it is closed. Then, the trivial inclusion $\mathbf{n}(\mathbf{B}'_i) \subseteq \mathbf{n}(\bar{\mathbf{B}}'_i)$ implies $\bar{\mathbf{n}}(\mathbf{B}'_i) \subseteq \mathbf{n}(\bar{\mathbf{B}}'_i)$. By definition we have $\bar{\mathbf{n}}(\mathbf{B}'_i) = \mathbf{n}(\mathbf{B}'_i) \cup \partial \mathbf{n}(\mathbf{B}'_i)$ with $\mathbf{n}(\mathbf{B}'_i) \cap \partial \mathbf{n}(\mathbf{B}'_i) = \emptyset$ and $\mathbf{n}(\bar{\mathbf{B}}'_i) = \mathbf{n}(\mathbf{B}'_i) \cup \mathbf{n}(\partial \mathbf{B}'_i)$. Then, the inclusion $\bar{\mathbf{n}}(\mathbf{B}'_i) \subseteq \mathbf{n}(\bar{\mathbf{B}}'_i)$ implies $\partial \mathbf{n}(\mathbf{B}'_i) \subseteq \mathbf{n}(\partial \mathbf{B}'_i)$. Since $\partial \mathbf{B}'_i \subseteq \mathbf{F}$, we have $\mathbf{n}(\partial \mathbf{B}'_i) \subseteq \mathbf{n}(\mathbf{F})$. One can then verify by direct computation that $\mathbf{n}(\mathbf{F}) \subseteq \mathbf{R}$, thus proving the thesis. ■

We now recall a result of basic topology which will be useful in the following.

Sublemma 3. Let A and B be open sets such that $\bar{A} \subseteq \bar{B}$. Then, there exists a point p such that $p \in \text{int} \bar{B}$ and $p \notin \bar{A}$.

Proof. Let us suppose that $B \subseteq \bar{A}$. Since B is open and \bar{A} is closed, we have $\bar{B} \subseteq \bar{A}$ which contradicts the hypothesis. ■

The following result will be of crucial importance.

Sublemma 4. The following identity holds:

$$\overline{\mathbf{n}(\mathbf{B}'_i)} = \bar{\mathbf{U}}. \quad (\text{B2})$$

Proof. First, we prove the easiest inclusion $\overline{\mathbf{n}(\mathbf{B}'_i)} \subseteq \bar{\mathbf{U}}$. From item 1 of Sublemma 2 we have that $\mathbf{n}(\mathbf{B}'_i) \subseteq \mathbf{n}(\bar{\mathbf{B}}'_i) \subseteq \bar{\mathbf{U}}$ (the first inclusion is trivial). Reminding that $\mathbf{n}(\mathbf{B}'_i)$ is open we have $\overline{\mathbf{n}(\mathbf{B}'_i)} \subseteq \bar{\mathbf{U}}$.

We now prove that $\bar{\mathbf{U}} \subseteq \overline{\mathbf{n}(\mathbf{B}'_i)}$. By contradiction, let us suppose that the strict inclusion $\overline{\mathbf{n}(\mathbf{B}'_i)} \subset \bar{\mathbf{U}}$ holds. Then, thanks to Sublemma 3, we find $p \in \bar{\mathbf{U}}$ such that $p \notin \overline{\mathbf{n}(\mathbf{B}'_i)}$. Moreover, we can find an open neighborhood \mathbf{N} of p such that $\mathbf{N} \cap \overline{\mathbf{n}(\mathbf{B}'_i)} = \emptyset$ and then without loss of generality we can suppose that $p \in \mathbf{Q}'$. Since \mathbf{R} has no interior points, $\mathbf{n}(\mathbf{B}'_i)$ cannot be included in \mathbf{R} , hence, $\mathbf{n}(\mathbf{B}'_i) \cap \mathbf{Q}'$ is not empty. Let us now fix a point $q \in \mathbf{n}(\mathbf{B}'_i) \cap \mathbf{Q}'$. Then, for any continuous path γ connecting p and q there exist t' such that $\gamma(t') \in \partial \mathbf{n}(\mathbf{B}'_i)$. From item 2 of Sublemma 2 we have $\gamma(t') \in \mathbf{R}$. Since this conclusion contradicts the fact that \mathbf{Q}' is connected, we have proved the thesis. ■

As a consequence, we have the following:

Corollary 1. The following inclusion holds $\mathbf{Q}' \subseteq \mathbf{n}(\mathbf{B}'_i)$.

Proof. From Sublemma 4 we have $\mathbf{Q}' \cup \mathbf{R} = \mathbf{n}(\mathbf{B}'_i) \cup \partial \mathbf{n}(\mathbf{B}'_i)$. Reminding that $\mathbf{Q}' \cap \mathbf{R} = \emptyset = \mathbf{n}(\mathbf{B}'_i) \cap \partial \mathbf{n}(\mathbf{B}'_i)$ and the inclusion $\partial \mathbf{n}(\mathbf{B}'_i) \subseteq \mathbf{R}$, proved in Sublemma 2, we have the thesis. ■

We now turn our attention to the regions \mathbf{B}'_i . Our first objective is to determine how many different \mathbf{B}'_i regions are. The answer is provided by the following result.

Sublemma 5. The regions \mathbf{B}'_i are in one-to-one correspondence with the solution of the equation $|\lambda(\mathbf{k})|^2 = 1$.

Proof. We proved that the map \mathbf{n}_i defines a diffeomorphism between \mathbf{B}'_i and the set $\mathbf{n}(\mathbf{B}'_i) \subseteq \bar{\mathbf{P}}$ which includes the origin. Then, for each \mathbf{B}'_i there exist a point \mathbf{k} such that $\mathbf{n}(\mathbf{k}) = 0$ and it is unique. Since $\mathbf{n}(\mathbf{k}) = 0$ if and only if $|\lambda(\mathbf{k})|^2 = |\lambda(\mathbf{k})|^2 - 1 = 0$, we have the thesis. ■

Thanks to this result it is sufficient to find the solutions of $|\lambda(\mathbf{k})|^2 = 1$ in the Brillouin zone. One can easily check that there are only four solutions and then four different regions $\mathbf{B}'_0, \dots, \mathbf{B}'_3$.

We can now prove the first part of Lemma 1.

Sublemma 6. The region \mathbf{B}'_i are given by

$$\begin{aligned} \mathbf{B}'_0 &:= \{\mathbf{k} \in \mathbf{B} | \lambda(\mathbf{k}) > 0, \cos(2k_y) > 0\}, \\ \mathbf{B}'_1 &:= \{\mathbf{k} \in \mathbf{B} | \lambda(\mathbf{k}) < 0, \cos(2k_y) > 0\}, \\ \mathbf{B}'_2 &:= \{\mathbf{k} \in \mathbf{B} | \lambda(\mathbf{k}) > 0, \cos(2k_y) < 0\}, \\ \mathbf{B}'_3 &:= \{\mathbf{k} \in \mathbf{B} | \lambda(\mathbf{k}) < 0, \cos(2k_y) < 0\}. \end{aligned} \quad (\text{B3})$$

Proof. Let us denote with $\bar{\mathbf{B}}_i$ the regions defined by the right-hand sides of Eq. (B3). One can immediately see that (i) the $\bar{\mathbf{B}}_i$ are open sets, (ii) the $\bar{\mathbf{B}}_i$ are mutually disjoint, and (iii) the union of the $\bar{\mathbf{B}}_i$ is the union of the \mathbf{B}'_i . We now prove that

for all \tilde{B}_i there exist a unique B'_j such that $\tilde{B}_i \subseteq B'_j$. This fact, together with the previous properties of the \tilde{B}_i , gives $\tilde{B}_i = B'_i$.

Clearly, for all \tilde{B}_i we must have $\tilde{B}_i \subseteq B'_{j_1} \cup \dots \cup B'_{j_k}$ for some $k \geq 1$. Let us suppose then that there exist \tilde{B}_i such that $\tilde{B}_i \subseteq B'_{j_1} \cup \dots \cup B'_{j_k}$ with k strictly greater than 1. Since we have as many \tilde{B}_i as B'_i , there must exist a B'_i and two points $\mathbf{k}_a \in \tilde{B}_a$ and $\mathbf{k}_b \in \tilde{B}_a$ such that $\mathbf{k}_a, \mathbf{k}_b \in B'_i$. Since B'_i is connected, there must exist a path connecting \mathbf{k}_a and \mathbf{k}_b that entirely lies within B'_i . On the other hand, since the \tilde{B}_i are disjoint, this path would cross the border of the \tilde{B}_a , but this contradicts the fact that the border of the \tilde{B}_a is not included in B'_i . ■

Finally, we can give the complete characterization of the sets $\mathbf{n}(B'_i)$. From Corollary 1 we have the inclusion $Q' \subseteq \mathbf{n}(B'_i)$. Since $|\mathbf{n}(\mathbf{k})| = 1 \iff \lambda(\mathbf{k}) = 0$, we know that the $S^2 \not\subseteq \mathbf{n}(B'_i)$. It is easy to check that also the points $p_{\pm} := (0, \pm \frac{\sqrt{2}}{2}, 0)$ are not included in the set $\mathbf{n}(B'_i)$. For any region $\mathbf{n}(B'_i)$, we will determine which ones of the eight open arches defined as

$$\begin{aligned} E_j^{\pm} &:= \mathbf{e}_{\pm}(L_j), \\ L_1 &:= (0, \frac{\pi}{2}), \quad L_2 := (\frac{\pi}{2}, \pi), \\ L_3 &:= (-\frac{\pi}{2}, 0), \quad L_4 := (-\pi, -\frac{\pi}{2}) \end{aligned} \quad (\text{B4})$$

are included in $\mathbf{n}(B'_i)$.

Let us consider the sets E_j^+ . If we for some t we have $\mathbf{n}(\mathbf{k}) = \mathbf{e}_+(t)$ and $\cos(2k_y) \neq 0$, then it must be

$$k_x = \frac{\pi}{4} + n\frac{\pi}{2}, \quad k_z = k_x + m\pi \quad (\text{B5})$$

for n and m integers. Equation (B5) then implies

$$\lambda(\mathbf{k}) = (-1)^m \frac{1}{2} [\cos(k_y) - \sin(k_y)]. \quad (\text{B6})$$

From Eq. (B6) we have

$$\lambda(\mathbf{k}) > 0 \implies \begin{cases} m \text{ even} \wedge -\frac{3}{4}\pi < k_y < \frac{1}{4}\pi, \\ m \text{ odd} \wedge \frac{1}{4}\pi < k_y < \frac{5}{4}\pi. \end{cases} \quad (\text{B7})$$

Then, if we assume $\mathbf{k} \in B'_0$ we must have

$$\begin{aligned} m \text{ even}, \quad & -\frac{1}{4}\pi < k_y < \frac{1}{4}\pi, \\ m \text{ odd}, \quad & \frac{3}{4}\pi < k_y < \frac{5}{4}\pi. \end{aligned} \quad (\text{B8})$$

However, since the two sets of \mathbf{k} are related by a translation of $(0, l\pi, l\pi)$, $l \in \mathbb{Z}$, they actually represent the same set in the Brillouin zone. So, it suffices to consider just the first set in Eq. (B8), that can be written as

$$\begin{aligned} k_x &= \frac{1}{4}\pi + n\frac{1}{2}\pi, \quad \frac{1}{4}\pi < k_y < \frac{1}{4}\pi, \\ k_z &= \frac{1}{4}\pi + n\frac{1}{2}\pi + m\pi = \frac{1}{4}\pi + n\frac{1}{2}\pi, \end{aligned} \quad (\text{B9})$$

where we used Eq. (B5) and in the second equality in the second line of Eq. (B9) we used the hypothesis that m is even. Using again the fact that we identify points related by a translation of $(l\pi, 0, l\pi)$, $l \in \mathbb{Z}$, we find just two inequivalent sets

$$Z_1 := \begin{cases} k_x = \frac{1}{4}\pi \\ \frac{1}{4}\pi < k_y < \frac{1}{4}\pi, \\ k_z = \frac{1}{4}\pi \end{cases}, \quad Z_2 := \begin{cases} k_x = -\frac{1}{4}\pi \\ \frac{1}{4}\pi < k_y < \frac{1}{4}\pi. \\ k_z = -\frac{1}{4}\pi \end{cases}.$$

It is now easy to show that the images of these two sets under the map \mathbf{n} are $\mathbf{n}(Z_1) = E_2^+$ and $\mathbf{n}(Z_2) = E_4^+$. By applying an analogous line of reasoning, one can prove all the following inclusions:

$$\begin{aligned} (E_2^+ \cup E_4^+ \cup E_1^- \cup E_3^-) &\subset \mathbf{n}(B'_0), \\ (E_1^+ \cup E_3^+ \cup E_2^- \cup E_4^-) &\not\subset \mathbf{n}(B'_0), \\ (E_2^+ \cup E_4^+ \cup E_1^- \cup E_3^-) &\subset \mathbf{n}(B'_2), \\ (E_1^+ \cup E_3^+ \cup E_2^- \cup E_4^-) &\not\subset \mathbf{n}(B'_2), \\ (E_1^+ \cup E_3^+ \cup E_2^- \cup E_4^-) &\subset \mathbf{n}(B'_1), \\ (E_2^+ \cup E_4^+ \cup E_1^- \cup E_3^-) &\not\subset \mathbf{n}(B'_1), \\ (E_1^+ \cup E_3^+ \cup E_2^- \cup E_4^-) &\subset \mathbf{n}(B'_3), \\ (E_2^+ \cup E_4^+ \cup E_1^- \cup E_3^-) &\not\subset \mathbf{n}(B'_3). \end{aligned} \quad (\text{B10})$$

This result completes the proof of Eq. (A7) of Lemma 1.

APPENDIX C: THE FUNCTION $g(\omega, \mathbf{m})$

In this appendix, we now show how it is possible to define a function $g(\omega, \mathbf{m})$ such that the map \mathcal{N} defines a diffeomorphism between \mathbf{N} and the null mass shell Γ_0 . The purpose of the following construction is to reduce the region \mathbf{N} to a star-shaped region $\tilde{\mathbf{N}}$ by removing a null-measure region, and to define the function $g(\omega, \mathbf{m})$ in such a way that the map \mathcal{N} is invertible on $\tilde{\mathbf{N}}$. Since multiplication by $g(\omega, \mathbf{m})$ rescales the four-vector $(\sin \omega, \mathbf{m})$ without affecting its direction, in order to have an invertible map \mathcal{N} it is sufficient to ensure that $g(\omega, \mathbf{m})$ is *radially monotonic* versus \mathbf{m} , namely, $g(\omega, r\mathbf{m}_0)$ must be monotonic versus r .

Let us denote E_{\pm} the ellipses defined by the parametric equations (A5). We define the polynomials

$$\begin{aligned} h_U(r, \theta, \phi) &:= 1 - r^2, \\ h_E(r, \theta, \phi) &:= [\cos^2(\phi) - \sin^2(\phi)]^2 \\ &\quad + \left\{ \frac{1}{2} - r^2 [1 - \cos^2(\theta) \sin^2(\phi)] \right\}^2, \end{aligned} \quad (\text{C1})$$

where we used the spherical coordinates $m_x = r \cos \theta \cos \phi$, $m_y = r \sin \theta$, $m_z = r \cos \theta \sin \phi$. Clearly, we have $h_U(\mathbf{m}), h_E(\mathbf{m}) > 0 \forall \mathbf{n} \in \mathbf{U}$, $h_U(\mathbf{m}) = 0 \iff \mathbf{m} \in S^2$, $h_E(\mathbf{m}) = 0 \iff \mathbf{m} \in E_+ \cup E_-$, and h_U, h_E are analytic on $\mathbf{U} \setminus \mathbf{H}$. Since $\mathbf{U} \setminus \mathbf{H}$ is star shaped, we can define

$$\tilde{g}(r, \theta, \phi) := r \int_0^r ds \left[\frac{1}{h_U(s, \theta, \phi)} + \frac{1}{h_E(s, \theta, \phi)} \right]. \quad (\text{C2})$$

The condition $h_U(\mathbf{m}), h_E(\mathbf{m}) > 0 \forall \mathbf{n} \in \mathbf{U} \setminus \mathbf{H}$ implies that the function $\tilde{g}(r, \theta, \phi)$ is radially monotonic on $\mathbf{U} \setminus \mathbf{H}$. Since $h_U(\mathbf{m})$ and $h_E(\mathbf{m})$ are analytic on $\mathbf{U} \setminus \mathbf{H}$ we have that $\tilde{g}(r, \theta, \phi)$ is analytic on $(\mathbf{U} \setminus \mathbf{H}) \setminus \mathbf{0}$. Moreover, since $\tilde{g}(r, \theta, \phi)$ is even in r we have that $\tilde{g}(\mathbf{m})$ is analytic on the whole domain $\mathbf{U} \setminus \mathbf{H}$. Finally, it is easy to check that $g(\mathbf{m})$ diverges to $+\infty$ as \mathbf{m} approaches the boundary of $\mathbf{U} \setminus \mathbf{H}$, and that $(\nabla g)(0) = \mathbf{0}$. Let us define

$$g(\mathbf{m}) := \tilde{g}(\mathbf{m}) + 1. \quad (\text{C3})$$

We now check that, with this definition of the map $g(\mathbf{m})$, the map \mathcal{N} defines an analytic diffeomorphism between $\mathbf{U} \setminus \mathbf{H}$ and Γ_0 with the property $J_{\mathcal{N}}(\mathbf{0}) = I$. Clearly, \mathcal{N} is analytic in \mathbf{N} so

we just need to prove that it gives a bijection between \mathbf{N} and Γ_0 . Let us fix a versor \mathbf{j} in \mathbb{R}^3 . Then, in the \mathbf{j} direction we have

$$\mathcal{N}(\omega, r\mathbf{j}) = g(r, \theta_{\mathbf{j}}, \phi_{\mathbf{j}}) \begin{pmatrix} \sin(\omega) \\ r\mathbf{j} \end{pmatrix}. \quad (\text{C4})$$

Since $g(r, \theta_{\mathbf{j}}, \phi_{\mathbf{j}})$ is monotone we clearly have that \mathcal{N} is injective. We now prove the surjectivity of $\mathcal{N}'(\omega, r) := \mathcal{N}(\omega, r\mathbf{j})$ on the set $\mathbf{K} := \{(p_0, p_1) \in \mathbb{R}^2 \text{ such that } p_0^2 - p_1^2 = 0\}$. Let us

fix a point $p = (p_0, p_1) \in \mathbf{K}$. Since $g(r, \theta_{\mathbf{j}}, \phi_{\mathbf{j}})$ is monotone and surjective on $[1, +\infty)$ we can find a value r_p such that $r_p g(r_p, \theta_{\mathbf{j}}, \phi_{\mathbf{j}}) = p_1$. Clearly, since $|r_p| < 1$, also the equation $\sin^2(\omega_p) = |r_p|^2$ can be solved and then $\mathcal{N}'(\omega_p, r_p) = (p_0, p_1)$. Since the surjectivity of \mathcal{N} holds for any direction \mathbf{j} , we have that \mathcal{N} is a diffeomorphism between \mathbf{N} and Γ_0 . Finally, since $g(\mathbf{0}) = 1$ and $\nabla g(\mathbf{0}) = \mathbf{0}$, we have that the Jacobian of the map \mathcal{N} is the identity, which proves Eq. (A11). Obviously, our choice of the map $g(\mathbf{m})$ is not unique.

[1] R. Feynman, *Int. J. Theor. Phys.* **21**, 467 (1982).
 [2] *Feynman and Computation*, edited by A. J. Hey (Perseus Books, Reading, MA, 1998).
 [3] J. Stachel, in *From Quarks to Quasars: Philosophical Problems of Modern Physics*, edited by R. G. Colodny and A. Coffa (University of Pittsburgh Press, Pittsburgh, 1986), pp. 349–81.
 [4] G. Immirzi, *Nucl. Phys. B, Proc. Suppl.* **57**, 65 (1997).
 [5] A. Perez, *Class. Quantum Grav.* **20**, R43 (2003).
 [6] L. Bombelli, J. Lee, D. Meyer, and R. D. Sorkin, *Phys. Rev. Lett.* **59**, 521 (1987).
 [7] A. Schild, *Phys. Rev.* **73**, 414 (1948).
 [8] G. Amelino-Camelia, *Phys. Lett. B* **510**, 255 (2001).
 [9] G. Amelino-Camelia, *Int. J. Mod. Phys. D* **11**, 35 (2002).
 [10] J. Magueijo and L. Smolin, *Phys. Rev. Lett.* **88**, 190403 (2002).
 [11] B. Schumacher and R. Werner, [arXiv:quant-ph/0405174](https://arxiv.org/abs/quant-ph/0405174).
 [12] P. Arrighi, V. Nesme, and R. Werner, *J. Comput. Syst. Sci.* **77**, 372 (2011).
 [13] D. Meyer, *J. Stat. Phys.* **85**, 551 (1996).
 [14] A. Ambainis, E. Bach, A. Nayak, A. Vishwanath, and J. Watrous, in *Proceedings of the Thirty-third Annual ACM Symposium on Theory of Computing* (ACM, New York, 2001), pp. 37–49.
 [15] G. M. D’Ariano and P. Perinotti, *Phys. Rev. A* **90**, 062106 (2014).
 [16] P. de La Harpe, *Topics in Geometric Group Theory* (University of Chicago Press, Chicago, 2000).
 [17] G. M. D’Ariano, M. Erba, P. Perinotti, and A. Tosini, [arXiv:1511.03992](https://arxiv.org/abs/1511.03992).
 [18] L. Susskind, *Phys. Rev. D* **16**, 3031 (1977).
 [19] G. Amelino-Camelia and T. Piran, *Phys. Rev. D* **64**, 036005 (2001).
 [20] G. M. D’Ariano, *Phys. Lett. A* **376**, 697 (2012).
 [21] L. Freidel, R. G. Leigh, and D. Minic, [arXiv:1606.01829](https://arxiv.org/abs/1606.01829).
 [22] M. Moyer, *Sci. Am.* **306**, 30 (2012).
 [23] C. J. Hogan, *Phys. Rev. D* **85**, 064007 (2012).
 [24] I. Pikovski, M. Vanner, M. Aspelmeyer, M. Kim, and C. Brukner, *Nat. Phys.* **8**, 393 (2012).
 [25] G. Amelino-Camelia, J. Ellis, N. E. Mavromatos, D. V. Nanopoulos, and S. Sarkar, *Nature (London)* **393**, 763 (1998).
 [26] A. Bisio, G. M. D’Ariano, and P. Perinotti, *Ann. Phys. (NY)* **368**, 177 (2016).
 [27] V. Vasileiou, J. Granot, T. Piran, and G. Amelino-Camelia, *Nat. Phys.* **11**, 344 (2015).
 [28] G. Amelino-Camelia, L. Freidel, J. Kowalski-Glikman, and L. Smolin, *Phys. Rev. D* **84**, 084010 (2011).